

# X-ray emission during the muonic cascade in hydrogen

B. Lauss,\* P.Ackerbauer, W.H.Breunlich, B.Gartner, M.Jeitler, P.Kammel,† J.Marton, W.Prymas, and J.Zmeskal  
*Institute for Medium Energy Physics, Austrian Academy of Sciences, Boltzmannngasse 3, A-1090 Wien, Austria*

D.Chatellard, J.-P.Egger, and E.Jeannet  
*Institut de Physique de l'Université, CH-2000 Neuchâtel, Switzerland*

H.Daniel, F.J.Hartmann, and A.Kosak  
*Physics Department, TU München, D-85747 Garching, Germany*

C.Petitjean  
*Paul Scherrer Institut, CH-5232 Villigen, Switzerland*  
(August 20, 2019)

We report our investigations of X rays emitted during the muonic cascade in hydrogen employing charge coupled devices as X-ray detectors. The density dependence of the relative X-ray yields for the muonic hydrogen lines ( $K_\alpha$ ,  $K_\beta$  and  $K_\gamma$ ) has been measured at densities between 0.00115 and 0.97 of liquid hydrogen density. In this density region collisional processes dominate the cascade down to low energy levels. A comparison with recent calculations is given in order to demonstrate the influence of Coulomb deexcitation.

Exotic atoms are atoms in which an electron is replaced by a heavier negatively charged particle, e.g.  $\mu^-$ ,  $\pi^-$ ,  $K^-$ ,  $\bar{p}$ . The simplest of these atoms is muonic hydrogen  $\mu p$ , which denotes a bound state of one proton and one muon.

After a free muon is injected into a hydrogen target it is slowed down and an excited muonic hydrogen atom is formed via Coulomb capture [1,2], leaving the muon most likely in an initial state of  $11 \leq n \leq 15$  [4]. This is the starting point for a complicated interplay of competitive collisional and radiative deexcitation processes, the so-called atomic cascade, which ends with the muonic atom being in the 1s ground state. The possibility of a metastable 2p state in muonic hydrogen is currently under investigation [3].

Muons, in contrast to the other possible particles, are not affected by strong interaction. So they may serve as the best probe for the investigation of these deexcitation processes.

At the investigated hydrogen densities, collisional deexcitation dominates from the beginning of the cascade to low n states, depending on the target density and the kinetic energy of the  $\mu p$  atom [1,5–8]. The known collisional processes are chemical dissociation, elastic collision, external Auger electron emission, Coulomb deexcitation and Stark mixing. The importance of the last two effects is due to the very small size of the neutral  $\mu p$  atom, which can penetrate very deeply into the electron cloud of a neighboring  $H_2$  molecule, where it can “feel” the electromagnetic field of the protons.

In the investigated hydrogen gases, the transitions to the ground state are always accompanied by the emission of muonic X rays; at liquid hydrogen density (LHD)<sup>‡</sup>, the X-ray emission probability is still 0.95 [7].

All these processes together make up the “standard cascade model” [1,5,6,9,10] which, despite its success, has one severe limitation: this is the assumption that  $\epsilon_{\mu p}$ , the kinetic energy of the  $\mu p$  atom, is constant throughout the cascade.

A recent calculation [7,8] tries to take into account the time evolution of  $\epsilon_{\mu p}$  for energy levels  $n \leq 6$ . Due to Coulomb deexcitation, complex energy distributions at various levels are expected. Coulomb deexcitation is the only known mechanism which can accelerate  $\mu p$  atoms up to epithermal energies of  $\sim 170$  eV [7]. In spite of its importance, Coulomb deexcitation is regarded as the least known process of the muonic cascade (neglecting chemical deexcitation, which is important only at very high energy levels) [8]. Existing calculations of the Coulomb deexcitation cross sections differ among themselves by more than one order of magnitude [11–15].

Apart from the basic interest in exotic atoms, the understanding of the deexcitation of muonic atoms is of great importance for various other phenomena, such as muon catalyzed fusion [16–18], muon transfer [19–21], diffusion of muonic atoms [22], and nuclear muon capture [23,24]. The muonic case can also be used as a test for the cascade in hadronic atoms [25] (e.g.  $\pi^- p$ ) where velocity effects [26,27] severely affect the evaluation of strong interaction parameters [28,29].

For this measurement, the relative X-ray yields of the emitted muonic hydrogen  $K^{\mu p}$  lines – the corresponding X-ray energies are  $K_\alpha = 1.90$  keV,  $K_\beta = 2.25$  keV,  $K_\gamma = 2.37$  keV and  $K_\infty = 2.53$  keV – and their intensity ratios

serve as a tool to investigate the muonic cascade.

This is the first systematic investigation of muonic X rays in this density region, and the first one which gives intensities for the three lowest muonic K lines. Earlier experiments [30–34] were either rather inaccurate or performed at very low gas densities ( $< 10^{-3}$  x LHD) only.

Our measurements were carried out with the high intensity muon beam of the  $\mu$ E4 area at PSI (Paul Scherrer Institut, Villigen, Switzerland). Figure 1 shows the setup for the measurements at liquid hydrogen density. Several different silver-coated steel or aluminum target cells were optimized for the measurements in liquid and gaseous hydrogen, respectively [35].

To minimize X-ray absorption, Kapton windows with a thickness of  $12.5 \mu\text{m}$  were used for the measurements at LHD. The gas target equipped with  $25 \mu\text{m}$  thick windows had to withstand pressures of up to 6 bar at temperatures around 30 K. For safety reasons, the target vacuum vessel was separated from the CCD’s vacuum with an additional  $12.5 \mu\text{m}$  Kapton window. The target cells were partly covered with superinsulation to reduce radiation heating.

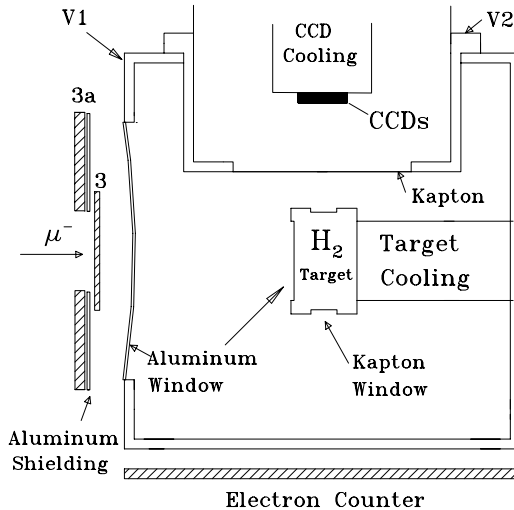


FIG. 1. Top view of the setup of this experiment. The displayed target cell was used for the measurements in liquid hydrogen. Two separated vacuum vessels were used; one for the target (V1), and one for the CCD-detector (V2). To ensure an optimal stopping efficiency the scintillation counters 3 and 3a were used to register incoming muons. The electron counter served to detect muon decay electrons. Larger target cells, adapted to the expected extent of the muon stopping distributions, were used for the measurements in gaseous hydrogen [35].

To avoid high Z impurities in the target, which would change the K line intensities through excited-state muon transfer [36,19], the hydrogen was cleaned during the filling procedure by using a liquid-nitrogen trap together with a palladium filter. The composition of the hydrogen was checked online during the measurements by using a quadrupole mass spectrometer [37] which could extract samples via a small capillary leading directly into the target volume. The stability of the target pressure and temperature was monitored and controlled during all measurements.

Charge coupled devices (CCDs) [38,39] have been employed as X-ray detectors. They consisted of two CCD sensors<sup>§</sup> with an active detection area of  $\sim 25 \times 17 \text{ mm}^2$  ( $\sim 880000$  pixels) for each chip. The main chip component was silicon with small absorption layers of  $\text{SiO}_2$  and  $\text{Si}_3\text{N}_4$  on the surface. The depletion thickness of  $\sim 30 \mu\text{m}$  was well adapted for the observed energy region. To shorten the readout time, each chip was split into two electronically independent detection areas.

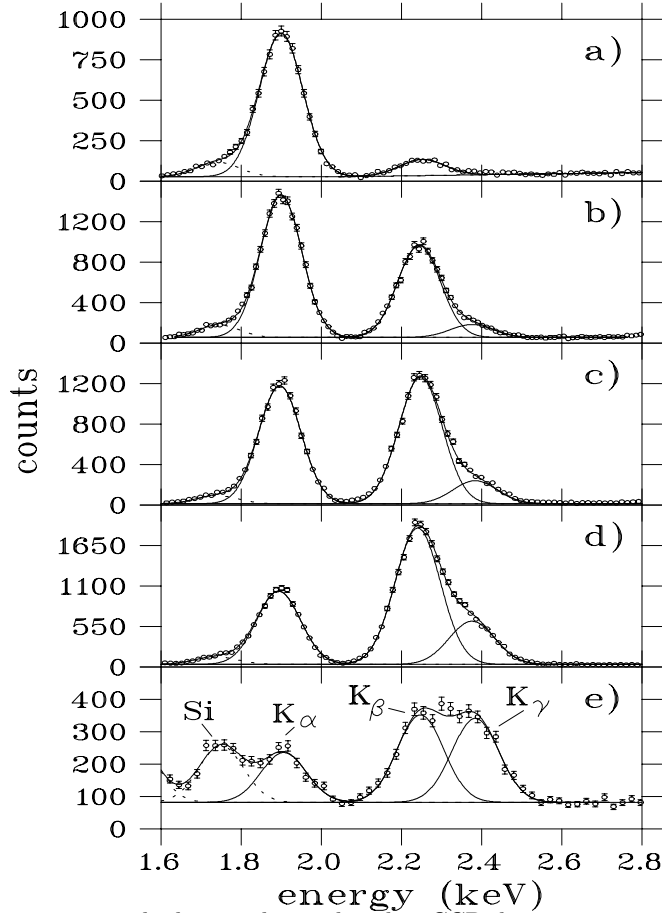


FIG. 2. Muonic X-ray energy spectra in hydrogen observed with a CCD-detector at temperatures of  $\sim 30$  K and various target densities  $\Phi$  (given in units of LHD): a)  $\Phi = 0.97$ , b)  $\Phi = 0.0795$ , c)  $\Phi = 0.0391$ , d)  $\Phi = 0.0106$ , e)  $\Phi = 0.00115$ .  $K_\alpha$ ,  $K_\beta$  and  $K_\gamma$  lines could be separated. The energy resolution of the detector  $\Delta E^{\text{FWHM}}/E$  at 2 keV was 6 %. The solid lines indicate Gaussian fits. The density dependence of the line intensities is clearly visible. The X-ray peak at 1.74 keV (dashed line) is due to fluorescence excitation of the detector’s silicon material. The low counting statistics in measurement e) reflects the already very low stopping probability of muons in such a low-density hydrogen gas.

We were able to apply a specific pattern recognition algorithm to separate “true” X-ray hits from charged particles and cosmic background using a “single pixel” selection criterion [40–42]. A “single pixel” was considered to be a “true” X ray if the charge content of the surrounding eight neighbor pixels was statistically compatible with the noise peak of the CCDs.

Data runs lasted for three minutes to guarantee that not more than  $\sim 15$  % of the CCD’s pixel were hit. A longer exposure time would have caused a decrease in the detection efficiency. A fraction of hit pixels of more than 30 % actually would have made it impossible to apply our selection criterion for X rays.

Our measurements investigated a density region covering three orders of magnitude. The observed raw energy spectra are displayed in fig.2. The intensity variation of the muonic hydrogen  $K_\alpha$ ,  $K_\beta$  and  $K_\gamma$  lines with target density can be seen directly. No K lines higher than  $K_\gamma$  could be observed.

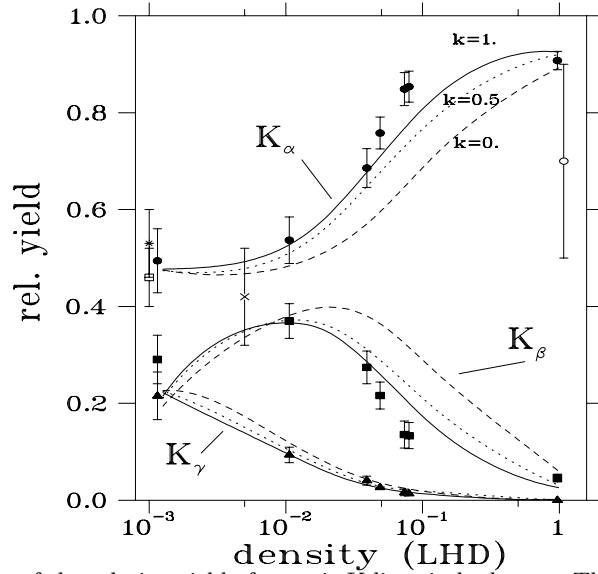


FIG. 3. The density dependence of the relative yield of muonic K lines in hydrogen. The measured relative yield is given as the number of counts in one K line ( $K_i$ ,  $i=\alpha, \beta, \gamma$ ) divided by the total count rate in all observed K lines ( $K_{\text{tot}}=K_\alpha+K_\beta+K_\gamma$ ). The plotted data points at LHD include a 5 % correction for non-radiative ground state transitions [7]. Filled circles, squares and triangles indicate the relative yield for  $K_\alpha$ ,  $K_\beta$  and  $K_\gamma$  transitions, respectively. The other experimental points for  $K_\alpha$  yields are taken from Refs. [30](cross), [31](open circle), [32](star) and [33] (square). The displayed calculated results from [8] used a scaling factor  $k$  for the Coulomb deexcitation cross section;  $k = 0$  (dashed line),  $k = 0.5$  (dotted line) and  $k = 1$  (full line).

An empty target run and a  $\mu^+$  run proved that there were no background peaks visible within the relevant energy region. The X-ray peak at 1.74 keV is due to fluorescence excitation of the detector's silicon material. Therefore the background function could be approximated by the sum of a constant and a term depending linearly on energy. Gaussians with energy-dependent width [35,40] were used to fit the peak areas.

The knowledge of the X-ray detection efficiency was indispensable for a correct analysis. A Monte Carlo program was written [35] to correctly account for the various contributions to X-ray absorption. The geometry of the different target cells, the absorption in the windows and in the CCDs' top layers was simulated. The intrinsic detection efficiency of the CCDs and the absorption in the Kapton foils were measured experimentally [35].

TABLE I. Results of the muonic X-ray measurements in hydrogen.

Density [LHD]	$K_\alpha/K_{\text{tot}}$	$K_\beta/K_{\text{tot}}$	$K_\gamma/K_{\text{tot}}$	$K_\alpha/K_\beta$
$0.9700 \pm 0.0050$	$0.952 \pm 0.019$	$0.048 \pm 0.008$	$0.000 \pm 0.010$	$19.92 \pm 2.45$
$0.0795 \pm 0.0008$	$0.854 \pm 0.032$	$0.133 \pm 0.027$	$0.013 \pm 0.006$	$6.41 \pm 1.25$
$0.0738 \pm 0.0008$	$0.849 \pm 0.034$	$0.135 \pm 0.028$	$0.016 \pm 0.007$	$6.27 \pm 1.75$
$0.0489 \pm 0.0004$	$0.758 \pm 0.033$	$0.216 \pm 0.028$	$0.026 \pm 0.007$	$3.51 \pm 0.52$
$0.0391 \pm 0.0003$	$0.686 \pm 0.040$	$0.274 \pm 0.034$	$0.040 \pm 0.009$	$2.50 \pm 0.42$
$0.0106 \pm 0.0001$	$0.539 \pm 0.048$	$0.369 \pm 0.036$	$0.092 \pm 0.016$	$1.46 \pm 0.25$
$0.00115 \pm 0.00005$	$0.494 \pm 0.041$	$0.291 \pm 0.050$	$0.215 \pm 0.049$	$1.70 \pm 0.38$

Figure 3 displays our results, given in Tab.I for the relative X-ray yields of the muonic hydrogen  $2 \rightarrow 1$ ,  $3 \rightarrow 1$  and  $4 \rightarrow 1$  transitions. The relative yield is given by the intensity of one specific K line ( $K_i$ ,  $i=\alpha, \beta, \gamma$ ) divided by the intensity of all observed K lines ( $K_{\text{tot}} = \sum_i K_i$ ). The plotted data at LHD include a 5 % correction for non-radiative ground state transfer according to [7]. This is the first measurement which allows us to test the existing cascade calculations at high target densities [5,7–9]. The calculations taken from [8] shown in fig.3 and fig.4 were done for different contributions of Coulomb deexcitation. The corresponding cross sections [11] were scaled with a factor  $k = 0$  (no contribution / dashed line),  $k = 0.5$  (dotted line) and  $k = 1$  (full line). The calculation according to the standard cascade model [5,9] coincides with the  $k = 0$  assumption. The displayed data – error bars include statistical errors and contributions due to efficiency corrections – match quite well the calculated density dependence. Though not very sensitive to  $k$  within the experimental errors, the yield measurements favor values of  $k \approx 1$ .

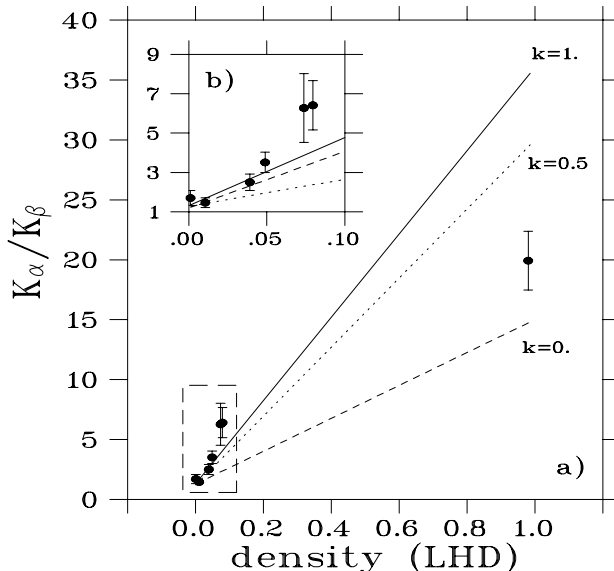


FIG. 4. a) The density dependence of the  $K_\alpha/K_\beta$  ratio in muonic hydrogen. The theoretical curves are calculated as in fig.3. b) displays the magnified low density region.

Theory [8] predicts that in the observed density region the density dependence of the  $K_\alpha/K_\beta$  ratio is approximately linear, with a significant contribution from Coulomb deexcitation. Figure 4 displays our results (Tab.I) together with the calculation from [8]. The  $K_\alpha/K_\beta$  value at LHD favors a scaling factor  $k < 0.5$ .

Although our measurements indicate that Coulomb deexcitation plays a significant role during the muonic cascade an unambiguous decision on the correct value of the scaling factor  $k$  is not yet possible.

The calculation of the relative line yields already seems to be quite reliable. However, the slight disagreement at 8 % of LHD could be an indication for a more complex density dependence of the collisional processes in the high density region; e.g. the existence of possible molecular effects [43]. Using a new calculation of the Coulomb deexcitation cross sections [15] in the cascade model could also explain the observed behavior and abolish the necessity of the scaling factor introduced in [8].

Financial support by the Austrian Science Foundation, the Austrian Academy of Sciences, the Swiss Academy of Sciences, the Swiss National Science Foundation and the German Federal Ministry of Research and Technology is gratefully acknowledged. It is a pleasure to thank D.Sigg for his software support and D.Varidel for his excellent technical assistance. Many fruitful discussions with E.C.Aschenauer and V.E.Markushin, who provided us with the results of their calculations prior to publication, are acknowledged.

\* E-Mail: Lauss@AMUON.IMEP.UNIVIE.AC.AT

† present address: University of California and L. Berkeley National Laboratory, Berkeley, CA 94720, USA.

‡ Liquid Hydrogen Density (LHD) =  $4.25 \times 10^{22}$  atoms/cm<sup>3</sup>.

§ Type CCD-05-20-1-207 by EEV (English Electric Valve), Waterhouse Lane, Chelmsford, Essex, England.

- [1] M.Leon and H.A.Bethe, Phys.Rev. 127, 636 (1962).
- [2] J.S.Cohen, R.L.Martin and W.R.Wadt, Phys.Rev.A Vol.27, 1821 (1983).
- [3] D.Taqqu *et al.*, Hyperfine Interact. 101/102, 599 (1996).
- [4] G.A.Fesenko and G.Ya.Korenman, *ibid.*, p.91.
- [5] M.Leon, Phys.Lett. 35b, 413 (1971).
- [6] V.E.Markushin, Zh. Eksp. Teor. Fiz. 80, 35 (1981), [Sov.Phys. JETP 53, 60 (1981)].
- [7] V.E.Markushin, Phys.Rev.A 50,2, 1137 (1994).
- [8] E.C.Aschenauer and V.E.Markushin., Hyperfine Interact. 101/102, 97 (1996), and Z.Phys. D 39, 165 (1997).
- [9] E.Borie and M.Leon, Phys.Rev.A 21,5, 1460 (1980).
- [10] F.Kottmann, in *Muonic Atoms and Molecules*, ed. by L.A.Schaller and C.Petitjean, (Birkhäuser, Basel, 1993), p.219.
- [11] L.Bracci and G.Fiorentini, Nuovo Cim. 43a, 9 (1978).
- [12] L.I.Men'shikov, Muon.Cat.Fus. 2, 173 (1988).
- [13] A.V.Kravtsov and A.I.Mikhaïlov, Zh. Eksp. Teor. Fiz. 107, 1473 (1995), [Sov.Phys. JETP 80, 822 (1995)], and Nukleonika 40, 25 (1995).
- [14] W.Czaplinski *et al.*, Phys.Rev.A 50, 525 (1995).
- [15] L.I.Ponomarev and E.V.Solov'ev, JETP Lett. 64, 135 (1996).
- [16] W.H.Breunlich, P.Kammel, J.S.Cohen and M.Leon, Annu.Rev.Nucl.Part.Sci. 39, 311 (1989).
- [17] J.Zmeskal *et al.*, Phys.Rev.A 42, 1165 (1990).
- [18] P.Kammel, Lett.Nuovo.Cim. 43, 349 (1985).
- [19] B.Lauss *et al.*, Phys.Rev.Lett. 76, 4693 (1996).
- [20] B.Lauss *et al.*, Hyperfine Interact. 101/102, 285 (1996).
- [21] B.Gartner *et al.*, *ibid.*, p.249.
- [22] D.J.Abbot *et al.*, Phys.Rev.A 55, 214 (1997).
- [23] W.H.Breunlich, Nucl.Phys.A 335, 137 (1980).
- [24] W.H.Breunlich, Nucl.Phys.A 353, 201c (1981).
- [25] T.P.Terada and R.S.Hayano, Phys.Rev.C 55, 73 (1997).
- [26] A.Badertscher *et al.*, Phys.Lett.B 392, 278 (1997).
- [27] E.C.Aschenauer *et al.*, Phys.Rev.A 51, 1965 (1995).
- [28] D.Chatellard *et al.*, Phys.Rev.Lett. 74, 4157 (1995).
- [29] D.Sigg *et al.*, Phys.Rev.Lett 75, 3245 (1995).
- [30] A.Placci *et al.*, Phys.Lett. 32B, 413 (1970)
- [31] B.Budick *et al.*, Phys.Lett. 34B, 539 (1971).
- [32] H.Anderhub *et al.*, Phys.Lett. 71B, 443 (1977).
- [33] P.O.Egan *et al.*, Phys.Rev.A 23, 1152 (1981).
- [34] H.Anderhub *et al.*, Phys.Lett. 143B, 65 (1984).
- [35] B.Lauss, Ph.D. thesis, University of Vienna 1997.
- [36] S.S.Gershtein, Zh. Eksp. Teor. Fiz. 43, 706 (1962), [Sov.Phys. JETP 16, 501 (1963)].
- [37] B.Gartner, Diploma thesis, University of Graz 1994.
- [38] D.Varidel *et al.*, Nucl. Instr. and Meth. A 292, 141 (1990).
- [39] G.Fiorucci *et al.*, *ibid.*, p.147.
- [40] J.-P.Egger, D.Chatellard and E.Jeannet, in *Muonic Atoms and Molecules*, ed. by L.A.Schaller and C.Petitjean, (Birkhäuser, Basel, 1993), p.331.
- [41] J.-P.Egger, D.Chatellard and E.Jeannet, Part. World Vol.3, 139 (1993).
- [42] D.Sigg, Nucl. Instr. and Meth. A 345, 107 (1994).
- [43] P.Froelich and J.Wallenius, Phys.Rev.Lett. 75, 2108 (1995).